The coupling between sister kinetochore directional instability and oscillations in centromere stretch in metaphase PtK1 cells

Xiaohu Wan, Daniela Cimini*, Lisa A. Cameron†, and E. D. Salmon
Biology Department, University of North Carolina, Chapel Hill, NC 27599

ABSTRACT **Kinetochores bound to kinetochore microtubules (kMTs) exhibit directional instability in mammalian and other mitotic vertebrate cells, oscillating between poleward (P) and away-from-the-pole (AP) movements. These oscillations are coupled to changes in length of kMTs in a way that maintains a net stretch of the centromere. To understand how sister kinetochore directional instability and kMT plus-end dynamic instability are coupled to oscillations in centromere stretch, we tracked at high resolution the positions of fluorescent kinetochores and their poles for oscillating chromosomes within spindles of metaphase PtK1 cells. We found that the kinetics of P and AP movement are nonlinear and different. By subtracting contributions from the poleward flux of kMTs, we found that maximum centromere stretch occurred when the leading kinetochore switched from depolymerization to polymerization, whereas minimum centromere stretch occurred on average 7 s after the initially trailing kinetochore switched from polymerization to depolymerization. These differences produce oscillations in centromere stretch at about twice the frequency of kinetochore directional instability and at about twice the frequency of centromere oscillations back and forth across the spindle equator.**

Monitoring Editor
Stephen Doxsey
University of Massachusetts

Received: Sep 8, 2011
Revised: Dec 15, 2011
Accepted: Jan 24, 2012

INTRODUCTION

Faithful segregation of replicated chromosomes is an essential cell function. Accurate segregation of sister chromatids occurs when one sister kinetochore becomes attached to kinetochore microtubules (kMTs) extending toward one pole and the second sister becomes attached to kMTs toward the opposite pole (chromosome biorientation; amphitelic kinetochores). Mammalian kinetochores typically have 20–25 kMTs, which form the core of kinetochore fibers extending between kinetochores and poles during metaphase (Rieder, 1981; McEwen *et al.*, 1997). Bioriented chromosomes with amphitelic kinetochores become aligned near the spindle equator at metaphase with their centromeres stretched by net pulling forces at sister kinetochores (Inoué and Salmon, 1995; Rieder and Salmon, 1998; Maiato *et al.*, 2004). Tension from centromere stretch is important for stabilizing kMT attachment (Nicklas *et al.*, 1998; Maiato *et al.*, 2004; Santaguida and Musacchio, 2009).

Bioriented chromosomes with amphitelic kinetochores in many mammalian tissue cells in culture exhibit three coupled oscillations at metaphase: oscillations in the distance of sister kinetochores from their poles, oscillations in the centroids of centromeres back and forth across the equator, and oscillations in the stretch of the centromere between sister kinetochores (Wan *et al.*, 2009; Jaqaman *et al.*, 2010). These oscillations are coupled to changes in kinetochore fiber length in a way that maintains a net stretch of the centromere; compression rarely occurs (Khodjakov and Rieder, 1996; Waters *et al.*, 1996a; Maiato *et al.*, 2004). Although poorly understood, the mechanisms producing these metaphase chromosome oscillations are important because they are produced by the same spindle and kinetochore mechanisms that control metaphase chromosome alignment and anaphase chromosome segregation (Maiato *et al.*, 2004). Not all amphitelic kinetochores at metaphase oscillate, and regular oscillations can switch to irregular movement (Magidson *et al.*, 2011). What causes the regular oscillations to stop is unknown. Chromosomes can also become bioriented near the

This article was published online ahead of print in MBoC in Press (http://www.molbiolcell.org/cgi/doi/10.1091/mbc.E11-09-0767) on February 1, 2012.

Present addresses: *Department of Biological Sciences, Virginia Tech, Blacksburg, VA 24061; †Dana-Farber Cancer Institute, Boston, MA 02215.

Address correspondence to: Xiaohu Wan (xwan@email.unc.edu).

Abbreviations used: kMT, kinetochore microtubule; MT, microtubule.

© 2012 Wan *et al.* This article is distributed by The American Society for Cell Biology under license from the author(s). Two months after publication it is available to the public under an Attribution–Noncommercial–Share Alike 3.0 Unported Creative Commons License (http://creativecommons.org/licenses/by-nc-sa/3.0).

"ASCB®," "The American Society for Cell Biology®," and "Molecular Biology of the Cell®" are registered trademarks of The American Society of Cell Biology.

Supplemental Material can be found at:
http://www.molbiolcell.org/content/suppl/2012/01/31/mbc.E11-09-0767v1.DC1.html

metaphase plate, with one or both sister kinetochores attached to kMTs extending from both poles (instead of just one), and these merotelic kinetochores do not oscillate or exhibit normal anaphase movements (Cimini *et al.*, 2004, 2006).

A number of factors are believed to contribute to oscillations of chromosomes with amphitelic kinetochores in vertebrate tissue cells: kinetochore directional instability (Skibbens *et al.*, 1993); poleward microtubule (MT) flux (Mitchison, 1989; Mitchison and Salmon, 1992); tension from stretch of the centromere produced by polar ejection forces on the chromosome arms, the relative movements of sister kinetochores, and/or kMT poleward flux (Rieder *et al.*, 1986; Skibbens *et al.*, 1993, 1995; Cassimeris *et al.*, 1994; Rieder and Salmon, 1994; Maddox *et al.*, 2003); and changes in protein concentration at kinetochores that depend on kinetochore fiber length (Varga *et al.*, 2006; Mayr *et al.*, 2007; Gardner *et al.*, 2008; Stumpff *et al.*, 2008; Du *et al.*, 2010; Jaqaman *et al.*, 2010) or kMT dynamic instability (Tirnauer *et al.*, 2002; Amaro *et al.*, 2010).

In this article, we investigate the dynamic features of kinetochore directional instability required for regular oscillations in centromere stretch for normal bioriented chromosomes within the middle of metaphase spindles in PtK1 mammalian tissue cells. Oscillations in centromere stretch have been poorly resolved in many previous studies that measured the kinetics of chromosome or kinetochore oscillations using phase or differential interference contrast microscopy to track the leading edges of the centromere region relative to the spindle poles (Skibbens *et al.*, 1993; Khodjakov and Rieder, 1996). More recent studies of oscillations within Ptk2 and human tissue cells tracked the position of fluorescent markers for kinetochores to improve the accuracy of locating the true position of the kinetochore (Wordeman *et al.*, 2007; Stumpff *et al.*, 2008; Dumont and Mitchison, 2009; Jaqaman *et al.*, 2010), but their kinetic analysis lacked information about the location of the spindle poles and about velocity variation during kinetochore P and AP movements. In addition, the kinetochore fibers in the HeLa cells studied are often highly curved and difficult to image between kinetochore and pole. PtK1 cells are much flatter than human cells and have much straighter kinetochore fibers. Accurate tracking of kinetochore movements relative to their fibers and to their poles and measurements of oscillation amplitude and frequency are necessary to understand the oscillation mechanism (Jaqaman *et al.*, 2010; Vladimirou *et al.*, 2011). We are able to measure kinetochore-to-pole distances by tracking different color fluorescent markers for kinetochores, spindle fibers, and poles. With this technology, we measured nonlinear kinetic profiles for kinetochore P and AP movements and key switch points in the dynamic instability of kMTs that appear necessary to produce the normal oscillation in centromere stretch at twice the frequency of kinetochore directional instability.

RESULTS

To label kinetochores and spindle poles, we microinjected PtK1 cells with a low dose of Alexa 488–labeled antibody to the peripheral kinetochore protein CENP-F and coinjected X-rhodamine–tubulin to label MTs. Injected cells exhibited normal progression through mitosis and accuracy in chromosome segregation (Cimini *et al.*, 2004, 2006; Cameron *et al.*, 2006). Time-lapse images were obtained at 15- or 20-s intervals at 35°C with a spinning disk confocal microscope to give high-contrast images and avoid effects of photobleaching (Figure 1A). A custom Matlab program was written to identify and track the centroids of fluorescent sister kinetochore pairs and the spindle poles (Figure 1B; Wan *et al.*, 2009; *Materials and Methods*). For each frame, the distance between kinetochores and their poles, the distance between the kinetochores and one pole, and the distance between sister kinetochore pairs were calculated from centroid *x*, *y* values (Figure 1, B and C).

At metaphase, chromosomes at the periphery of the spindle exhibited erratic movements but no continuous oscillations (Figure 1D; Cameron *et al.*, 2006; Cimini *et al.*, 2006), whereas chromosomes in the middle of the spindle exhibited nearly continuous oscillations (Figure 1, E and F, and Supplemental Movie S1). Within a given cell, the interkinetochore (K-K) centromere length of both nonoscillating and oscillating chromosomes became stretched beyond a rest length of ~1.1 μm (Hoffman *et al.*, 2001) to a similar average value (Figure 1D). In Figure 2, we plot for each cell analyzed the average K-K distance for both nonoscillating and oscillating bioriented chromosomes. Both increase with mitotic progression, and the average K-K centromere length of nonoscillating kinetochores is ~1.28 times the average and 0.93 times the peak values exhibited by oscillating kinetochores (Figure 2). At metaphase, sister kinetochores of both nonoscillating and oscillating kinetochores are pulled poleward by the same average rate of kMT poleward flux, ~0.65 μm/min (Cameron *et al.*, 2006). The reason chromosomes at the periphery of the spindle do not oscillate is unknown. It may depend on weaker polar ejection forces (Levesque and Compton, 2001) or high concentrations of the kinesin 8, Kif18A, at these kinetochores due to their long kinetochore fibers (Stumpff *et al.*, 2008). However, this study will focus on the oscillating chromosomes in the middle of the spindle.

Oscillations in centromere stretch occur at twice the frequency of kinetochore directional instability

To compare the oscillation in K-K centromere stretch to that of kinetochore directional instability, the discrete Fourier transform was applied to each sister kinetochore-to-pole distance and their K-K separation (Figure 3). Sister kinetochores oscillated at the same frequency, with a period close to 4 min/cycle (Figures 1, E and F, and 3, A and B). The same period was exhibited for chromosome oscillations back and forth across the spindle equator, as measured by the position of the center of the centromere between sister kinetochores (Figure 1F). In contrast, centromere stretch oscillated with a period of ~2 min/cycle, or twice the frequency of kinetochore-to-pole and chromosome oscillations (Figures 1, E and F, and 3).

K-K centromere oscillation at twice the frequency of kinetochore directional instability requires asymmetric P and AP kinetics

To investigate which kinetic parameters of kinetochore directional instability double the frequency of K-K centromere stretch, we generated simulations with different waveforms for P and AP movements (Supplemental Figure S1). For kinetochore oscillations with sinusoidal kinetics (Supplemental Figure S1A) or symmetric triangular wave kinetics where P and AP movement exhibit similar constant velocity, as reported for newt spindles (Skibbens *et al.*, 1993; Ke *et al.*, 2009; Supplemental Figure S1B), the frequency of K-K centromere oscillation was the same as for kinetochore directional instability regardless of the phase difference between the oscillations of the sister kinetochores (unpublished data). Further simulations (Supplemental Figure S1C) showed that K-K oscillations at twice the frequency of kinetochore-to-pole oscillations can occur for constant-velocity kinetic profiles of P and AP movement as long as they are sufficiently asymmetric (different velocities and durations of movement) and out of phase, as occurs in vivo (Figure 1, D and F). This result indicates that asymmetry in the kinetics of P and AP movement is critical for doubling the frequency of K-K centromere oscillations relative to kinetochore directional instability.

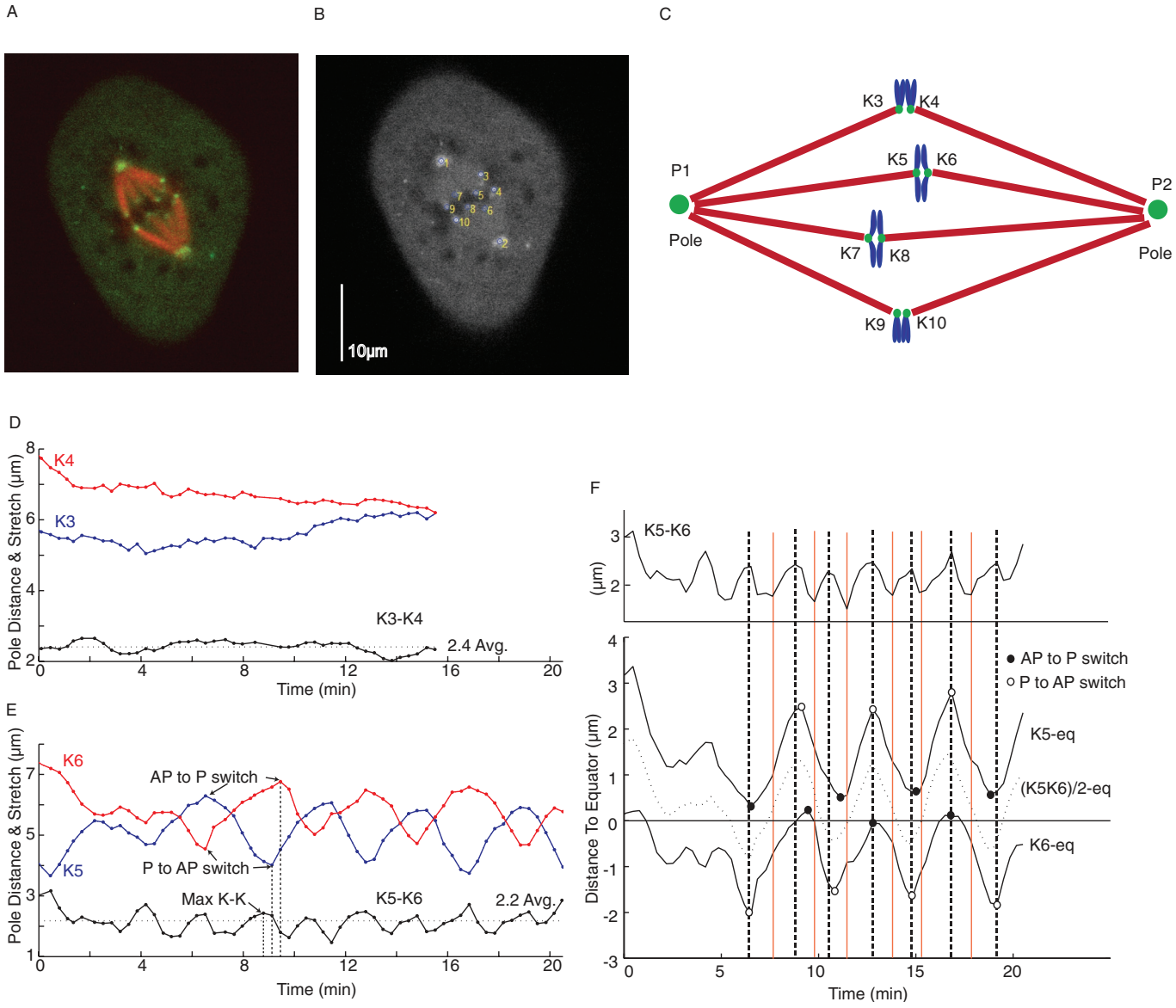

FIGURE 1: Measurements of normal kinetochore and centromere oscillations for bioriented chromosomes in metaphase spindles of PtK1 cells. (A) PtK1 cell with fluorescently labeled kinetochores (green), spindle poles (green), and MTs (red). (B) Image of spindle in our Matlab analysis interface with labeled kinetochores and poles selected for time-lapse motion analysis of fluorescent centroid positions. (C) Spindle diagram with labels used for kinetochores and spindle poles in our measurements. Plots of kinetochore-to-pole distance (in red and blue) and K-K distance (in black) between sister kinetochores for two nonoscillating chromosomes at the spindle periphery (D) and two oscillating sister kinetochores in the same cell (E). Switch points on K-P curves and maximum K-K distance were recorded (see E). The time resolution (15–20 s) did not allow detailed analysis of the switch in directional instability to determine whether the switch is instantaneous or there is a pause around the switch point. If such a pause exists, the switch point would correspond to the mid time point of the pause period. (F) Kinetic plots for the oscillating sister pair in D, identifying switches in direction of movement (open and closed circles) relative to the maximum (black vertical lines) and minimum (red vertical lines) points in K-K centromere stretch and the position of the center of the centromere between sister kinetochores (dotted curve). Top, plot of K-K distance. Bottom, plots of sister kinetochore positions and the center of the centromere relative to the spindle equator calculated from (P2 – P1)/2.

Kinetochore P and AP movements in PtK1 cells are nonlinear and different

In PtK1 cells, we found that the kinetic profiles of P and AP movement were very nonlinear, as shown for the average kinetic profiles for P and AP movements in Figure 4, A and B. There was also a large variation in velocity during P and AP movements (Figure 4, C and D) not exhibited by kinetochore directional instability in newts (Skibbens *et al.*, 1993; Ke *et al.*, 2009). In addition, both the kinetic profiles and velocity profiles during P and AP movement were distinctly different (Figure 4). For example, after a switch to P movement, the now leading kinetochore gradually reaches its maximum velocity poleward and then gradually slows before it switches direction to AP movement. In contrast, upon switching to AP movement, the kinetochore quickly reaches maximum speed and then slows

	P movement (n = 161)		AP movement (n = 161)	
Metaphase	Average	SD	Average	SD
Average velocity (μm/min)	1.14	0.35	0.94	0.28
Average distance (μm)	1.91	0.68	1.82	0.69
Average duration (min)	1.71	0.44	2	0.69
	Depolymerization/polymerization phases (assuming kMT poleward flux at 0.65 μm/min)			
	Depolymerization (n = 97)		Polymerization (n = 87)	
Metaphase	Average	SD	Average	SD
Average distance (μm)	1.17	0.42	3.61	0.85
Average duration (min)	1.47	0.37	2.55	0.73
Metaphase				
Average nonoscillating K-K distance	2.22 μm			
Average oscillating K-K distance	2.05 μm			
Average oscillating K-K max distance	2.44 μm			
Average oscillating K-K min distance	1.62 μm			
	P movement (n = 19)		AP movement (n = 19)	
Monotelic	Average	SD	Average	SD
Average velocity (μm/min)	1.27	0.48	1.06	0.35
Average distance (μm)	1.76	0.48	1.7	0.55
Average duration (min)	1.49	0.48	1.68	0.5
	P movement (n = 87)		AP movement (n = 89)	
Prometaphase	Average	SD	Average	SD
Average velocity (μm/min)	1	0.37	0.78	0.27
Average distance (μm)	1.32	0.6	1.22	0.61
Average duration (min)	1.38	0.56	1.56	0.63

P movement occurs for a slightly longer distance each cycle compared with AP movement. This is because there is a slow shortening of the pole-to pole distance typical of late prometaphase and metaphase cells (LaFountain, 1972; Cimini *et al.*, 2004).

TABLE 1: Measurements of P and AP movement for metaphase, prometaphase, and monopolar spindles.

gradually during the remainder of AP movement (Figure 4, C and D).

For kinetochore directional instability in metaphase PtK1 cells, the average velocity of P movement is ~20% faster than the average velocity of AP movement (1.1 vs. 0.9 μm/min, respectively, a difference that is statistically significant; Table 1). The average duration of P movement is ~20% shorter than AP movement, but the distances traveled in P movement and AP movement are on average about equal (Table 1).

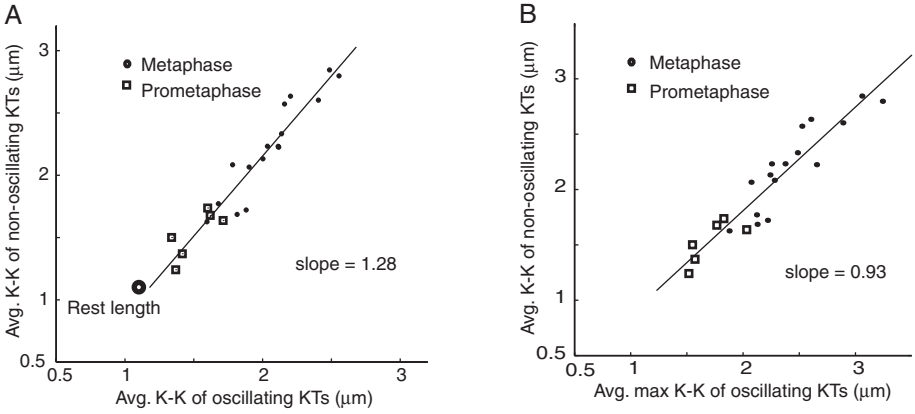

FIGURE 2: Average and maximum K-K centromere stretch for normally bioriented chromosomes increases with mitotic progression. Average (A) and maximum (B) K-K centromere stretch for oscillating kinetochores, as well as nonoscillating kinetochores, plotted for each cell analyzed in prometaphase (open squares) through metaphase (solid circles). The rest length of the centromere is ~1.1 μm in cells treated with nocodazole to inhibit MT assembly (Hoffman *et al.*, 2001). The solid lines are a least-squares fit through the data.

These major features of the nonlinear kinetics of kinetochore directional instability observed for bioriented chromosomes at metaphase were also observed for bioriented chromosomes in late prometaphase cells, where a few chromosomes had not become bioriented and congressed to the spindle equator (Supplemental Figure S2 and Table 1), and for mono-oriented chromosomes within monopolar spindles with one attached kinetochore (monotelic; Supplemental Figure S3 and Table 1). The only major differences between metaphase and prometaphase were a ~30% shorter period and a ~20% shorter distance traveled during oscillations (Table 1) and a ~25% decrease in the average centromere stretch (Figure 2). All the similarities in the nonlinear kinetic profiles of kinetochore P and AP movement between monopolar and bipolar

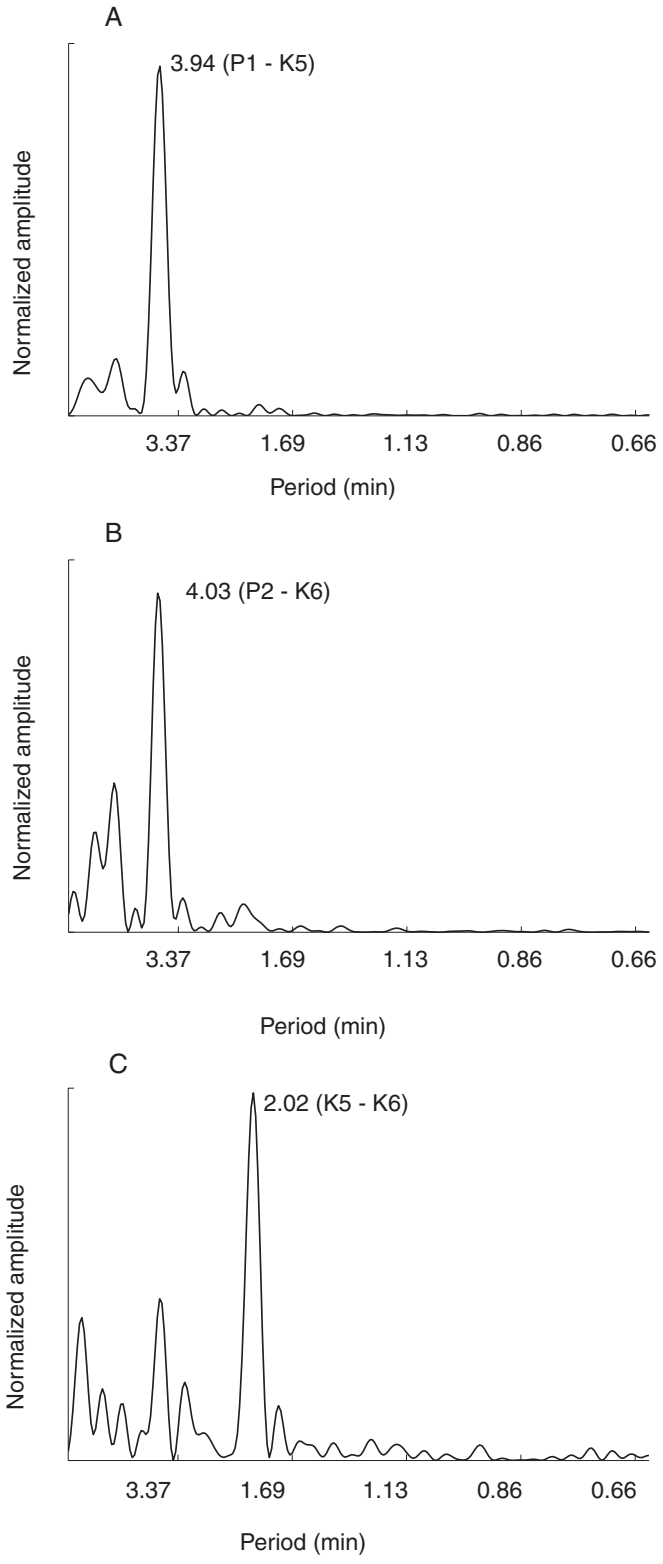

FIGURE 3: K-K centromere oscillations occur with half the period of kinetochore-to-pole oscillations. Fourier transform analysis of kinetochore-to-pole oscillations (A, B) and K-K oscillation (C) for the oscillating kinetochore pair in Figure 1, E and F. In each graph, the peak value represents the oscillation period. The peaks in A and B indicate the oscillation period of a sister kinetochore pair. Both values of oscillation in A and B are near 4 min. The peak in C shows K-K oscillation for the sister kinetochores in A and B. The value in C is ~2 min.

spindles show that the basic mechanisms responsible for the nonlinear kinetics are likely intrinsic to the polar MT arrays and the kinetochore, including how well dynamic instability is synchronized for the ~25 kMTs.

MT poleward flux makes the kinetics of kMT plus-end dynamic instability different from kinetochore directional instability in several ways

Without kMT poleward flux, switching between the depolymerization and polymerization phases occurs at the same time as switching between P and AP movements, respectively. This is because the relative movement of the kMT plus end to the pole is the same relative movement to the MT lattice. Also, force generation coupled to kMT depolymerization is the only mechanism moving the kinetochore poleward. However, the presence of kMT poleward flux at 0.65 μm/min average velocity in metaphase PtK1 cells makes the situation more complex (Cameron *et al*., 2006), as illustrated in Supplemental Figure S4F for time points labeled 1–10 in Figure 5. In Figure 5, oscillations in kinetochore P and AP movements relative to a pole are compared with cycles of kMT plus-end depolymerization and polymerization measured relative to the MT lattice. The depolymerization and polymerization cycles were obtained by adding the constant flux rate of 0.65 μm/min to the kinetics of kinetochore-to-pole movement. Although fluorescence speckle analysis showed that the flux rate varies, the average value of flux rate remains constant regardless of the lateral position of the kMT fiber (inner or outer), the polymerization or depolymerization states, and the centromere stretch (Cameron *et al*., 2006; Dumont and Mitchison, 2009). As a result, when the rate of polymerization at a kinetochore initially exhibiting AP movement slows to <0.65 μm/min, the kinetochore remains in the polymerization phase but switches to P movement because the polymerization rate becomes slower than the poleward flux velocity (Figure 5, point C at ~6 min). When the kinetochore subsequently switches to depolymerization (Figure 5, point A at ~7 min), P velocity becomes much faster, reaching a peak in the middle of P movement and then slows. The kinetochore switches from slow depolymerization to slow polymerization (Figure 5, point B at ~8 min), but the kinetochore persists in P movement until the rate of polymerization accelerates to exceed the rate of poleward flux (Figure 5, point D at ~ 8.5 min). Then the kinetochore switches into AP movement. At that time, the velocity of polymerization rapidly increases, producing a rapid increase in kinetochore AP velocity to a maximum rate. A similar pattern is repeated for subsequent cycles of kinetochore-to-pole oscillation, but the intervals between switches in phases and switches in directions are variable (Figure 5).

Overall, the combination of gradual transitions between states of kMT plus-end polymerization and depolymerization and poleward flux of kMTs at an average of 0.65 μm/min leads to the following: 1) AP-to-P switches occur before switching from polymerization to depolymerization; 2) P-to-AP switches occur after switching from depolymerization to polymerization; 3) the duration of depolymerization is shorter than P movement; 4) the duration of polymerization is longer than AP movement; and 5) the average depolymerization rate of kMTs is slower than their average polymerization rate.

kMT plus-end dynamics is correlated with centromere K-K oscillation

We measured the average times for switching between P and AP and polymerization and depolymerization relative to the time when the centromere reaches its maximum and minimum stretch (Table 2). Maximum K-K centromere stretch was achieved most

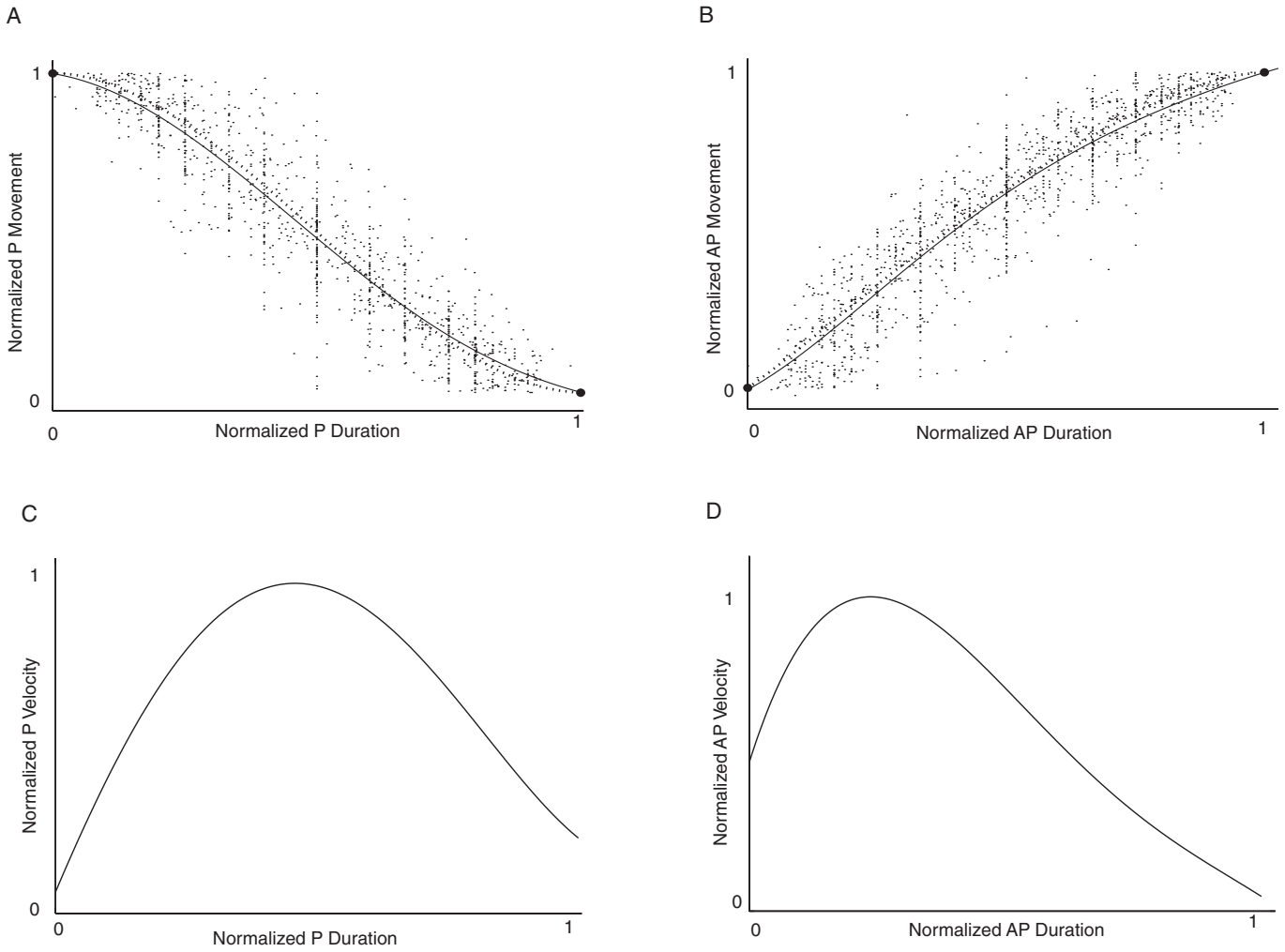

FIGURE 4: Kinetochore P and AP movements are not linear and different. Kinetic profiles of normalized P (A) and AP (B) movement. For each P or AP movement between two adjacent switch points (e.g., open and closed circles in Figure 1F), the individual kinetochore-to-pole distance trajectory was extracted. Each trajectory was then scaled so it began at 0 and ended at 1 in both displacement and time, and then these normalized curves were all plotted together on the same axes. Because the number of data points from an individual trajectory was limited by the frame interval, the data points from different trajectories were random samples of P and AP movements. On average they presented all the time points for both P and AP movements, not just a few separate ones limited by the frame interval. The scattering of the data points was largely contributed by the differences in motion among the populations of P and AP movements. The solid lines through the kinetic data in A and B were obtained by nonlinear least-squares fitting with no constraints on velocity at the beginning and end of the movements; the dotted lines were constrained to zero velocity at the beginning and end of P movement and the end of AP movement as described in the text. Polynomial curve fitting was used to obtain the average kinetic profiles. Norm of residuals of both P and AP curves (2.9 for both) was significantly smaller than the norm of residuals of linear fitting (3.2 for P and 3.5 for AP), indicating that curve fitting was better than linear fitting. Normalized P (C) and AP (D) velocity kinetics were obtained from the derivatives of the polynomial curves in A and B, respectively. During P movement (C), the kinetochore slowly gains velocity, achieving peak velocity in the middle of the movement and then slowing down before switching to AP movement. During AP movement (D), the kinetochore rapidly reaches peak velocity and then slows to nearly zero before switching to P movement. In our experiments, the image acquisition rate was not high enough to capture the transient moment at both the beginning and the end of P and AP movement. Such sampling error made the velocities from the derivatives at those points close but not equal to zero. Constrained fitting solved such problem (dotted lines in A and B; see the text for details).

often when the leading kinetochore switched from depolymerization to polymerization (*t* test, $p > 0.05$). In contrast, on average the switch from P to AP for the initially leading kinetochore lagged 0.15 min behind the time of maximum centromere stretch (*t* test, $p < 0.01$). After the initially leading kinetochore switched to AP movement, the trailing kinetochore did not immediately switch to P movement. On average, there was a 0.13-min lag before it switched to P movement (*t* test, $p < 0.01$) and became the leading kinetochore and a 0.39-min lag before it switched to depolymerization (*t* test, $p < 0.01$) and substantially increased P velocity. The initially trailing kinetochore switched to the depolymerization phase on average 0.14 min before the minimum in centromere K-K stretch (*t* test, $p < 0.01$). It is worth noting that the standard deviations for the different switch points relative to the time of

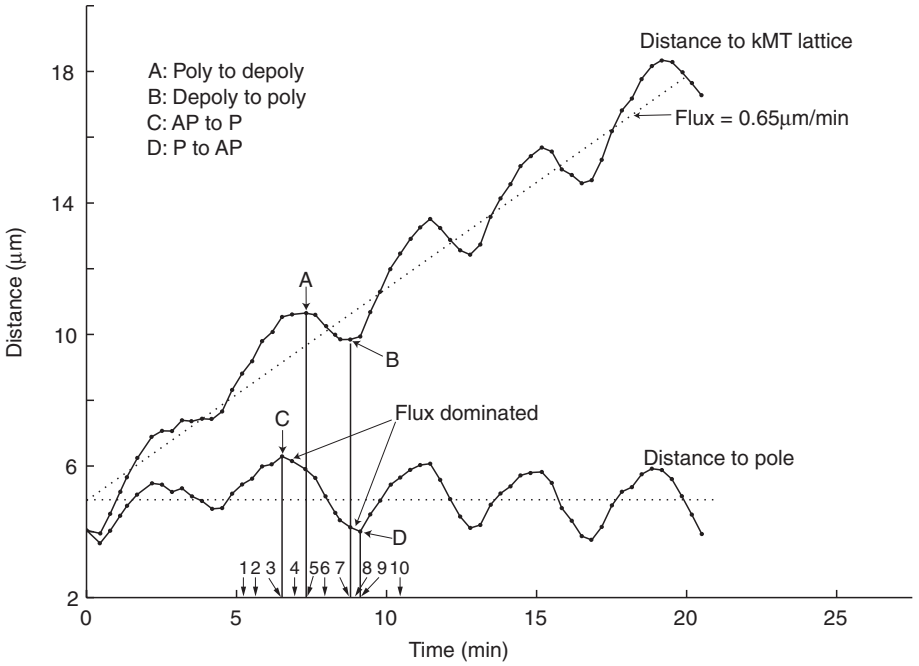

FIGURE 5: MT poleward flux makes the kinetics of kMT plus-end dynamic instability different from kinetochore directional instability. The kinetics of depolymerization and polymerization (top) were obtained by adding the constant flux rate of 0.65 μm/min to data for kinetics of kinetochore-to-pole movement (bottom). The average slope of repetitive phases of kMT plus-end depolymerization and polymerization is 0.65 μm/min, the net polymerization rate from kMT poleward flux. In contrast, the average slope of kinetochore directional instability is about zero. Both the velocities of polymerization and depolymerization slow down before switching to the other phase. A and B indicate switch points, and the labels 1–10 along the *x*-axis correspond to schematic diagrams in Supplemental Figure S4F.

maximum K-K stretch were large (Table 2), indicating that all the switches were very stochastic.

	Measurement results (min)	Simulation results (min)	
		Unconstrained fitting	Constrained fitting
Maximum KK	0	0	0
Leading depoly to poly	0.05 (±0.27)	–0.15	–0.05
Leading P to AP	0.15 (±0.30)	0.04	0.15
Trailing AP to P	0.28 (±0.45)	0.17	0.28
Trailing poly to depoly	0.54 (±0.22)	0.36	0.47
Minimum KK	0.68 (±0.21)	0.77	0.68

Measurements from experimental data and simulations of leading and trailing kinetochore switches between P and AP movements and switches between net polymerization (poly) and net depolymerization (depoly) relative to the maximum and minimum in K-K centromere stretch are shown. Simulations of constrained fitting (set velocity to zero at the beginning and end of P movement and at the end of AP movement) and unconstrained fitting are compared. The trailing polymerization-to-depolymerization switch time of 0.54 (±0.22) min was derived from subtracting its switch time of 0.14 (±0.22) min before minimum KK from the time between minimum and maximum KK.

TABLE 2: Timing of switches between P and AP and switches between polymerization and depolymerization relative to the maximum and minimum K-K distance.

Kinetic features of sister kinetochore directional instability that double the frequency of K-K centromere oscillations

We used computer simulations to generate plots of sister kinetochore directional instability and associated oscillations in K-K centromere stretch (Figure 6A) based on the average kinetochore profiles of kinetochore P and AP movement (Figure 4, A and B) and the average switching times (Table 2). Two types of simulation were performed. The first used kinetic profile curve fitting with no velocity constraints at the start and the end of P and AP movements (solid lines in Figure 4, A and B). The second constrained the curve fitting to yield zero velocities at the beginning and end of P movement and at the end of AP movement (dotted lines in Figure 4, A and B), which produced the velocity profiles in Figure 6B for P and AP movement. The simulation based on the constrained curve fits (Figure 6A) matched better the measured switching data (Table 2). This result also indicates that the curve fitting in Figure 4 is close to the average P and AP profiles.

In the diagrams in Figure 6, C and D, we provide a detailed description of how, on average, K-K centromere oscillations occur at about twice the frequency of sister kinetochore directional instability, based on our kinetic and switching time measurements. The magnitudes of kinetochore velocity (lengths of arrows) are derived from the P and AP velocity profiles in Figure 6B for metaphase cells, and the times for switching between P and AP movement and between depolymerization/polymerization phases are from Table 2. To start, the left sister kinetochore is leading and pulling the center of the centromere across the spindle equator. At that time there is increasing centromere stretch because the P velocity of the leading kinetochore is greater than the AP velocity of the trailing kinetochore. At the time of maximum centromere stretch (set to zero time on the vertical axis), the P velocity of the leading kinetochore has decreased to equal the AP velocity of the trailing kinetochore. Shortly afterward (0.05 min), the leading kinetochore switches from net depolymerization to net polymerization, but the initial rate of polymerization is less than the poleward flux rate of kMTs, and the leading kinetochore continues in P movement. Because the trailing kinetochore is moving faster in AP movement, the K-K centromere stretch decreases. At 0.15 min, the rate of net polymerization has increased above the rate of flux, and therefore the leading kinetochore switches to AP movement, increasing the rate at which K-K centromere stretch is reduced, since now both sisters are exhibiting AP movement. The initially trailing kinetochore switches from AP to slow P movement at 0.28 min because the net rate of polymerization has decreased to less than the flux rate. The K-K stretch of the centromere continues to decrease because the AP velocity of the initially leading sister kinetochore is larger than the P velocity of initially trailing kinetochore. The initially trailing kinetochore switches to depolymerization at 0.54 min when the P velocity becomes greater than the flux velocity. At 0.68 min, the AP velocity of the initially leading kinetochore has decreased and the P velocity of the

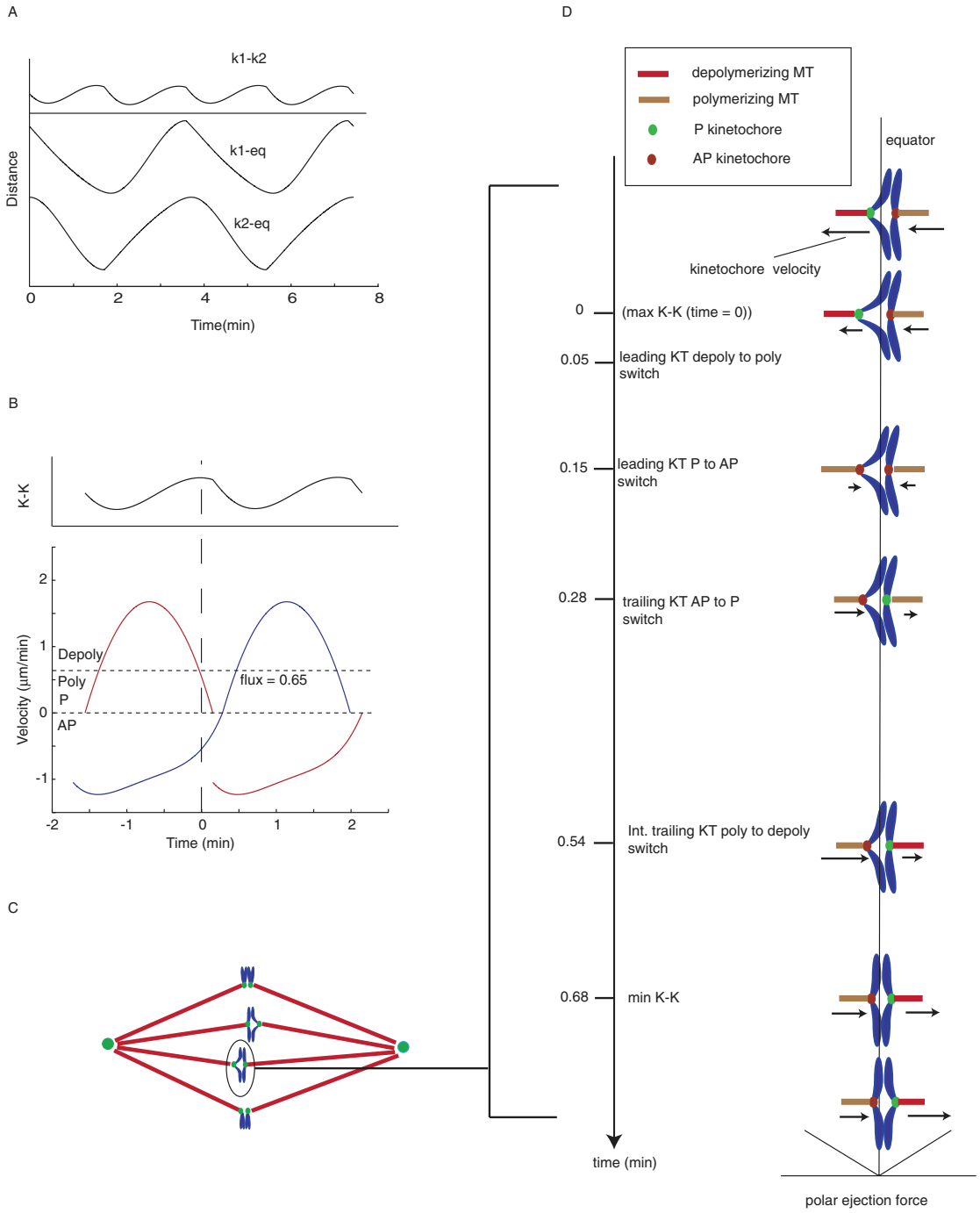

FIGURE 6: Kinetic features of sister kinetochore directional instability that double the frequency of K-K centromere oscillations compared with the frequency of oscillation of sister kinetochores and the center of the centromere in metaphase PtK1 cells. (A) Reconstruction of sister kinetochore oscillation relative to the equator and K-K oscillation based on the velocities in B. (B) Reconstructions of P and AP velocities for a pair of sister kinetochores (in blue and red). AP end velocity and P start and end velocities were constrained to zero for average kinetic profiles of P and AP movement (dotted lines in Figure 4). Only AP start velocity was not constrained. Average times for maximum and minimum K-K centromere stretch were obtained from Table 2. (C) Diagram of metaphase PtK1 cells. (D) Diagrammatic representation of half cycle of K-K centromere stretch for an oscillating chromosome, such as the one circled in (C). The half cycle begins before maximum stretch (time set equal to zero on the left-hand vertical axis) and ends just after minimum stretch. Initially, the left sister kinetochore is in depolymerization phase moving P and is the leading kinetochore pulling the sister pair across the equator (vertical line) and into the left half-spindle. The right sister kinetochore is the trailing kinetochore in polymerization phase and moving AP. The average times of switching between depolymerization/polymerization phases and P/AP movements are given on the left time axis as measured in Table 2. The average magnitudes of P and AP velocities as a function of time are indicated by the length of the arrows next to each kinetochore. Net polar ejection force, which increases with distance from the equator (assumed linear here), is shown at the bottom. See the text for more details.

initially trailing kinetochore increased to equal each other, so there is no longer a change in K-K centromere stretch, and a minimum is reached. Subsequently, the AP velocity of the initially leading kinetochore decreases and the P velocity of the initially trailing kinetochore increases, enhancing the K-K centromere stretch and beginning another half cycle in K-K centromere oscillation.

Note that at the minimum K-K centromere length, ~1.6 µm on average (Table 1), the centromere is still stretched above the rest-length of ~1.1 µm measured in the presence of nocodazole (Hoffman *et al.*, 2001). The K-K centromere length was less than the 1.1 µm rest length for only 1% of the time in metaphase and 4% in prometaphase. The average K-K values below the rest length in both metaphase and prometaphase were above 1 µm and very close to the rest length. This means that the centromere is rarely compressed, and an AP kinetochore normally does not actually push the centromere when it comes closer to the P kinetochore, as reported earlier for newt cells (Waters *et al.*, 1996b).

DISCUSSION

What produces the nonlinear kinetic profiles of kinetochore directional instability in PtK1 tissue cells?

There are four potential sources for the nonlinear kinetic and velocity profiles that differ between P and AP movement in PtK1 cells. One is the difference in force generation at kinetochores in phases of depolymerization and polymerization. In depolymerization, the force at the kinetochore is the active force coupled to MT depolymerization minus a resistive force produced by the movement of the kMT plus-end attachment sites poleward over the MT lattice. In polymerization in PtK1 cells, there is only a resistive force (Khodjakov and Rieder, 1996; Maddox *et al.*, 2003; Maiato *et al.*, 2004). The resistive forces at kinetochores are produced by the dynamics of nonmotor and motor protein links, such as the Ndc80 complex, cytoplasmic dynein, or CENP-E, to the lattice of kMT within kinetochore attachment sites (Maddox *et al.*, 2003). The resistive forces may be different in magnitude between depolymerizing and polymerizing kinetochores.

A second source is a dependence of P and AP velocity on centromere tension in PtK1 cells that is not seen in newt cells or grasshopper spermatocytes, where kinetochore P velocity appears to be "load independent" (Skibbens *et al.*, 1993, 1995; Skibbens and Salmon, 1997; Cassimeris *et al.*, 1994; Nicklas *et al.*, 1998). For the leading kinetochore in PtK1 cells, the P velocity becomes slowest at the end of P movement, when centromere stretch is near a maximum. Conversely, the AP velocity is highest near maximum centromere stretch (Figure 1, E and F). In this regard, Akiyoshi *et al.* (2010) recently showed that increasing tension applied to isolated yeast kinetochore complexes attached to the plus ends of pure tubulin MTs produces a moderate increase in the polymerization velocity and a substantial decrease in depolymerization velocity.

Third, there are factors whose concentration at kinetochores are proposed to increase with kinetochore fiber length. One such factor in human cells is Kif18A. Kif18A slows polymerization and depolymerization of MT plus ends (Stumpff *et al.*, 2008; Du *et al.*, 2010; Jaqaman *et al.*, 2010). This would help produce the reduction in AP velocity of the trailing kinetochore toward the end of AP movement—a reduction that would promote centromere stretch by the P movement of the leading kinetochore and increase tension at the leading kinetochore. When the trailing kinetochore switches from polymerization to depolymerization, Kif18A and other factors that had accumulated at kMT plus ends during polymerization could be responsible for the initially slow rate of kinetochore P movement. The time for removal of these factors from near the ends of kMTs after the onset of depolymerization may account for why the P velocity slowly increases to a maximum in the middle of P movement before tension from centromere stretch begins to slow velocity back down. Dumont and Mitchison (2009) found that increasing normal metaphase spindle length by compression does not alter kinetochore directional instability or average K-K distance. This result suggests that the length of a kinetochore fiber that controls the concentration of factors like Kif18a at a kinetochore is less than or equal to the normal length of kinetochore fibers at metaphase.

A fourth source is the synchronization in switching for the multiple kMT ends within the kinetochore. Switches in PtK1 cells are not nearly as abrupt as occurs for kinetochore directional instability in newt cells (Skibbens *et al.*, 1993), and yet both cell types have similar average metaphase numbers of kMTs (~24; Rieder, 1981; Cassimeris *et al.*, 1990). Electron microscopy of PtK1 kinetochores fixed in either P or AP movement shows more kMT plus ends classified as depolymerizing than as polymerizing (Maiato *et al.*, 2006; VandenBeldt *et al.*, 2006). This suggests that the velocity profiles during P and AP movement may be the result of "unsynchronized" changes in the number of depolymerizing versus polymerizing kMT ends. In this regard, in PtK1 cells we could not find any significant difference in the lateral width of kinetochore fluorescence (related to number of kMTs; Rieder, 1981) between nonoscillating kinetochores of chromosomes at the periphery of PtK1 spindles and oscillating kinetochores of chromosomes within the middle of the spindle.

Why does average centromere stretch for bioriented chromosomes increase from prometaphase to metaphase?

We propose that each occupied kMT binding site at a kinetochore produces a unit of force (active pulling during depolymerization; resistive pulling during polymerization; Hays and Salmon, 1990; Khodjakov *et al.*, 1997; Maddox *et al.*, 2003). The half-life of kMTs increases from prometaphase to metaphase (Zhai *et al.*, 1995; McEwen *et al.*, 1997; Cimini *et al.*, 2006; DeLuca *et al.*, 2006), resulting in an increase in occupancy of kMT attachment sites between prometaphase and metaphase (McEwen *et al.*, 1997, 1998). This increase in occupancy correlates with the increase in average centromere stretch (Figure 2). During the initial prometaphase congression of chromosomes to the equator in PtK1 cells the situation is different. Kinetochore force appears to be dependent not only on kMT number (Khodjakov and Rieder, 1996), but also on MT motor proteins, such as cytoplasmic dynein and CENP-E, that concentrate at kinetochores with few or no kMTs (Hoffman *et al.*, 2001; Kapoor *et al.*, 2006; Cai *et al.*, 2009).

What controls switching between net depolymerization and net polymerization phases?

The mechanisms controlling switching within kMT attachment sites are a major unsolved and controversial issue. Our data are consistent with the tension-dependent "slip clutch" mechanism (Skibbens *et al.*, 1993, 1995; Rieder and Salmon, 1994; Maddox *et al.*, 2003). In this model, the probability of switching from depolymerization to polymerization increases sharply at high tension similar to the response of force-induced dissociation of two proteins or unfolding of a protein (Skibbens *et al.*, 1995). Conversely, the probability of switching from polymerization to depolymerization increases sharply at low tension, in order to let two proteins associate or a domain to refold by their thermal motion. Experimental data in newts clearly show that P-to-AP switches depend on polar ejection forces (Skibbens *et al.*, 1995; Ke *et al.*, 2009). For purified budding yeast kinetochores attached to the plus ends of pure tubulin microtubules in vitro, high tension promotes rescue of depolymerizing ends back to polymerization and inhibits

catastrophe, the switch from polymerization to depolymerization (Akiyoshi *et al.*, 2010). However, the tension model fails by itself to explain why depleting the chromokinesin Kid stops metaphase kinetochore oscillations in human cells (Levesque and Compton, 2001), why chromosomes at the periphery of PtK1 cells do not exhibit regular oscillations while their centromeres are stretched to a similar average length (Figure 2B), and why depleting Kif18A in HeLa cells causes a major decrease in the average K-K centromere stretch, an increase in kinetochore velocities, and an increase in the extent of kinetochore oscillations away from the equator (Stumpff *et al.*, 2008; Jaqaman *et al.*, 2010).

We found that the initially trailing kinetochore almost always switches first to net depolymerization and P movement when both sisters are moving AP (Figure 6D). Both the lower tension from polar ejection forces near the equator and higher Kif18A concentration may work together to ensure that the initially trailing kinetochore switches first.

A major unanswered question is how cooperative switching is produced among the ~24 kMT attachment sites in kinetochores exhibiting regular oscillations, although a number of models have been proposed (Khodjakov and Rieder, 1996; Joglekar and Hunt, 2002; Maiato *et al.*, 2004; Liu *et al.*, 2008; Amaro *et al.*, 2010; Vladimirou *et al.*, 2011). Uncoordinated switching among attachment sites would stop persistent durations and regular oscillations typical of kinetochore directional instability (e.g., merotelic kinetochores; Cimini *et al.*, 2004). Oscillations in kinetochore protein composition, like that reported for CENP-H and CENP-I (Amaro *et al.*, 2010; Vladimirou *et al.*, 2011), or oscillations in kinase activity could control switching if their activity was regulated by stretch of the centromere proximal to a kinetochore or by tension-induced changes in intrakinetochore stretch (Santaguida and Musacchio, 2009; Maresca and Salmon, 2010). It will be interesting to see how all these potential mechanisms integrate together to coordinate the cooperative switching of kMT plus ends between depolymerization and polymerization states to produce K-K centromere oscillations at twice the frequency of kinetochore directional instability.

MATERIALS AND METHODS

Cell culture, microinjection, and microscopy

PtK1 cells were maintained in Ham's F-12 medium (Sigma-Aldrich, St. Louis, MO) complemented with 10% fetal bovine serum, antibiotics, and antimycotic and grown at 37°C, in a humidified incubator with 5% CO_2. For experiments, PtK1 cells were grown on acid-washed, sterilized coverslips in 35-mm Petri dishes. Microinjection and live-cell imaging of metaphase PtK1 cells were performed as described (Cimini *et al.*, 2004, Cameron *et al.*, 2006). The kinetochore marker was Alexa 488–labeled antibody to CENP-F, a peripheral kinetochore protein. MTs were labeled by microinjection of X-rhodamine–labeled tubulin.

We used a Nikon TE300 inverted microscope with a Yokogawa spinning disk confocal CSU10 unit (PerkinElmer Life Sciences Wallac, Gaithersburg, MD) to acquire time-lapse images through a 60× or 100×/1.4 numerical aperture Plan Apochromatic differential interference contrast objective lens. The camera was an Orca ER cooled CCD (Hamamatsu Photonics, Bridgewater, NJ). We used an argon/krypton laser and 488- and 568-nm filters in an excitation filter wheel (Sutter Instruments, Novato, CA). Sequential 488- and 568-nm fluorescence images were acquired every 15–20 s for one focal plane using MetaMorph software (Molecular Devices, Sunnyvale, CA). Exposure time was 500–1000 ms. The camera's pixel scale is 0.107 μm/pixel (no binning; 60×) and 0.13 μm/pixel (2 × 2 binning; 100×). Stage temperature was maintained at 35°C using an air curtain incubator (ASI 400; Nevtek, Williamsville VA).

Kinetochore detection

A customized software program was developed in Matlab (MathWorks, Natick, MA) to detect and track the positions of the kinetochores. Images acquired during the experiments were first loaded into the program. Then they were processed with a Gaussian smooth filter to suppress the background noise. The pixels with the highest intensity values among their neighbors in the processed images were identified as candidates. Only those pixel intensity values that were above a certain threshold were chosen as valid detections. Lowering the threshold would result in the detection of more kinetochores that were less bright but would also pick up background noise as signals. The program parameters allowed adjustment of the threshold level to identify as many kinetochores as possible without introducing too much noise.

Kinetochore localization

Kinetochore position was first represented by the *x*, *y* coordinates of the pixel with maximum brightness. The more accurate position of the kinetochore was then obtained by the two-dimensional (2D) Gaussian fitting method. The original image of the kinetochore, generally the size of a 9 pixel by 9 pixel region, was fitted by a 2D Gaussian function using a least-squares curve-fitting method to find the centroid of the signal. The *lsqcurvefit* function of Matlab was used to conduct the fitting. The centroid was used as the localization of the kinetochore. This method allowed subpixel accuracy. Localization of the pole position was identified using similar approaches when the pole was visible. If the pole was out of focus, its localization was determined by the converging point of the kMT fibers.

Kinetochore tracking

A nearest-neighbor method was used to track the kinetochore over time. The program searches the closest point in the following frame within a certain radius. The tracking was performed automatically, but editing functions were built into the program to allow visual correction of any tracking errors. In addition, tracks could be joined, cut, or terminated.

Kinetochore switch point

The distance between kinetochores and their corresponding attached poles along with the distance between the sister kinetochores was calculated using the centroid positions obtained as described. On the kinetochore-to-pole distance curve, local minimum and local maximum points were selected as kinetochore switch points. Local minimum points were P-to-AP switch points. Local maximum points were AP-to-P switch points. Local minimum and maximum points were also recorded from the kinetochore-to-kinetochore distance curve. A *t* test was performed on the time difference between two events by Matlab functions ttest and ttest2.

Oscillation frequency

Using the Matlab *fft* function, we performed a Fourier transform on both the kinetochore-to-pole distance data and the kinetochore-to-kinetochore distance data to obtain the oscillation frequency. The primary peak frequency of the Fourier transform result was taken as the oscillation frequency.

Simulations of oscillations

Simulations of kinetochore oscillations were generated with different wave forms using Matlab software (Supplemental Figure S1).

Wave forms include sine wave, symmetric triangle wave, and asymmetric triangle wave. Two waves were used in each simulation, showing the motion of sister kinetochore oscillations. The waves also represented the distance between the pole and kinetochore. To simplify the simulation, sister kinetochores were put on the pole-to-pole axis. Similar amplitude and period values (Table 1) from real kinetochore oscillations were used in all the simulated wave forms. The kinetochores were positioned in such a way that AP-to-P switches occurred near the equator. The K-K distance was then calculated to show the oscillation frequency. The simulation of in vivo kinetochore oscillations used the P and AP kinetic profiles (Figure 4, A and B). Oscillation amplitude and period (Table 1), as well as the position of the kinetochores, were implemented as described, except that the relative position of the sister kinetochore directional instability was adjusted to achieve the average centromere stretch value of ~2.2 µm.

ACKNOWLEDGMENTS

We thank A. Tsahai Tafari and Don Cleveland (University of California, San Diego, La Jolla, CA) for the gift of Alexa 488–labeled antibody to CENP-F. We also thank Gul Civelekoglu-Scholey and Sophie Dumont for comments and suggestions on the manuscript. This work was supported by a National Institutes of Health Grant (GM24364) to E.D.S.

REFERENCES

Akiyoshi B, Sarangapani KK, Powers AF, Nelson CR, Reichow SL, Arellano-Santoyo H, Gonen T, Ranish JA, Asbury CL, Biggins S (2010). Tension directly stabilizes reconstituted kinetochore-microtubule attachments. Nature 468, 576–579.

Amaro AC, Samora CP, Holtackers R, Wang E, Kingston IJ, Alonso M, Lampson M, McAinsh AD, Meraldi P (2010). Molecular control of kinetochore-microtubule dynamics and chromosome oscillations. Nat Cell Biol 12, 319–329.

Cai S, O'Connell CB, Khodjakov A, Walczak CE (2009). Chromosome congression in the absence of kinetochore fibres. Nat Cell Biol 11, 832–838.

Cameron LA, Yang G, Cimini D, Canman JC, Kisurina-Evgenieva O, Khodjakov A, Danuser G, Salmon ED (2006). Kinesin 5-independent poleward flux of kinetochore microtubules in PtK1 cells. J Cell Biol 173, 173–179.

Cassimeris L, Rieder CL, Rupp G, Salmon ED (1990). Stability of microtubule attachment to metaphase kinetochores in PtK1 cells. J Cell Sci 96, 9–15.

Cassimeris L, Rieder CL, Salmon ED (1994). Microtubule assembly and kinetochore directional instability in vertebrate monopolar spindles: implications for the mechanism of chromosome congression. J Cell Sci 107, 285–297.

Cimini D, Cameron LA, Salmon ED (2004). Anaphase spindle mechanics prevent mis-segregation of merotelically oriented chromosomes. Curr Biol 14, 2149–2155.

Cimini D, Wan X, Hirel CB, Salmon ED (2006). Aurora kinase promotes turnover of kinetochore microtubules to reduce chromosome segregation errors. Curr Biol 16, 1711–1718.

DeLuca JG, Gall WE, Ciferri C, Cimini D, Musacchio A, Salmon ED (2006). Kinetochore microtubule dynamics and attachment stability are regulated by Hec1. Cell 127, 969–982.

Du Y, English CA, Ohi R (2010). The kinesin-8 Kif18A dampens microtubule plus-end dynamics. Curr Biol 20, 374–380.

Dumont S, Mitchison TJ (2009). Compression regulates mitotic spindle length by a mechanochemical switch at the poles. Curr Biol 19, 1086–1095.

Gardner MK *et al.* (2008). Chromosome congression by kinesin-5 motor-mediated disassembly of longer kinetochore microtubules. Cell 135, 894–906.

Hays TS, Salmon ED (1990). Poleward force at the kinetochore in metaphase depends on the number of kinetochore microtubules. J Cell Biol 110, 391–404.

Hoffman DB, Pearson CG, Yen TJ, Howell BJ, Salmon ED (2001). Microtubule-dependent changes in assembly of microtubule motor proteins and mitotic spindle checkpoint proteins at PtK1 kinetochores. Mol Biol Cell 12, 1995–2009.

Inoué S, Salmon ED (1995). Force generation by microtubule assembly/disassembly in mitosis and related movements. Mol Biol Cell 6, 1619–1640.

Jaqaman K *et al.* (2010). Kinetochore alignment within the metaphase plate is regulated by centromere stiffness and microtubule depolymerases. J Cell Biol 188, 665–679.

Joglekar AP, Hunt AJ (2002). A simple, mechanistic model for directional instability during mitotic chromosome movements. Biophys J 83, 42–58.

Kapoor TM, Lampson MA, Hergert P, Cameron L, Cimini D, Salmon ED, McEwen BF, Khodjakov A (2006). Chromosomes can congress to the metaphase plate before biorientation. Science 311, 388–391.

Ke K, Cheng J, Hunt AJ (2009). The distribution of polar ejection forces determines the amplitude of chromosome directional instability. Curr Biol 19, 807–815.

Khodjakov A, Cole RW, McEwen BF, Buttle KF, Rieder CL (1997). Chromosome fragments possessing only one kinetochore can congress to the spindle equator. J Cell Biol 136, 229–240.

Khodjakov A, Rieder CL (1996). Kinetochores moving away from their associated pole do not exert a significant pushing force on the chromosome. J Cell Biol 135, 315–327.

LaFountain JR Jr (1972). Spindle shape changes as an indicator of force production in crane-fly spermatocytes. J Cell Sci 10, 79–93.

Levesque AA, Compton DA (2001). The chromokinesin Kid is necessary for chromosome arm orientation and oscillation, but not congression, on mitotic spindles. J Cell Biol 154, 1135–1146.

Liu J, Desai A, Onuchic JN, Hwa T (2008). An integrated mechanobiochemical feedback mechanism describes chromosome motility from prometaphase to anaphase in mitosis. Proc Natl Acad Sci USA 105, 13752–13757.

Maddox P, Straight A, Coughlin P, Mitchison TJ, Salmon ED (2003). Direct observation of microtubule dynamics at kinetochores in *Xenopus* extract spindles: implications for spindle mechanics. J Cell Biol 162, 377–382.

Magidson V, O'Connell CB, Lončarek J, Paul R, Mogilner A, Khodjakov A (2011). The spatial arrangement of chromosomes during prometaphase facilitates spindle assembly. Cell 146, 555–567.

Maiato H, DeLuca J, Salmon ED, Earnshaw WC (2004). The dynamic kinetochore-microtubule interface. J Cell Sci 117, 5461–5477.

Maiato H, Hergert PJ, Moutinho-Pereira S, Dong Y, Vandenbeldt KJ, Rieder CL, McEwen BF (2006). The ultrastructure of the kinetochore and kinetochore fiber in *Drosophila* somatic cells. Chromosoma 115, 469–480.

Maiato H, Rieder CL, Khodjakov A (2004). Kinetochore-driven formation of kinetochore fibers contributes to spindle assembly during animal mitosis. J Cell Biol 167, 831–840.

Maresca TJ, Salmon ED (2010). Welcome to a new kind of tension: translating kinetochore mechanics into a wait-anaphase signal. J Cell Sci 123, 825–835.

Mayr MI, Hummer S, Bormann J, Gruner T, Adio S, Woehlke G, Mayer TU (2007). The human kinesin Kif18A is a motile microtubule depolymerase essential for chromosome congression. Curr Biol 17, 488–498.

McEwen BF, Ding Y, Heagle AB (1998). Relevance of kinetochore size and microtubule-binding capacity for stable chromosome attachment during mitosis in PtK1 cells. Chromosome Res 6, 123–132.

McEwen BF, Heagle AB, Cassels GO, Buttle KF, Rieder CL (1997). Kinetochore fiber maturation in PtK1 cells and its implications for the mechanisms of chromosome congression and anaphase onset. J Cell Biol 137, 1567–1580.

Mitchison TJ (1989). Polewards microtubule flux in the mitotic spindle: evidence from photoactivation of fluorescence. J Cell Biol 109, 637–652.

Mitchison TJ, Salmon ED (1992). Poleward kinetochore fiber movement occurs during both metaphase and anaphase-A in newt lung cell mitosis. J Cell Biol 119, 569–582.

Nicklas RB, Campbell MS, Ward SC, Gorbsky GJ (1998). Tension-sensitive kinetochore phosphorylation in vitro. J Cell Sci 111, 3189–3196.

Rieder CL (1981). The structure of the cold-stable kinetochore fiber in metaphase PtK1 cells. Chromosoma 84, 145–158.

Rieder CL, Davison EA, Jensen LC, Cassimeris L, Salmon ED (1986). Oscillatory movements of monooriented chromosomes and their position relative to the spindle pole result from the ejection properties of the aster and half-spindle. J Cell Biol 103, 581–591.

Rieder CL, Salmon ED (1994). Motile kinetochores and polar ejection forces dictate chromosome position on the vertebrate mitotic spindle. J Cell Biol 124, 223–233.

Rieder CL, Salmon ED (1998). The vertebrate cell kinetochore and its roles during mitosis. Trends Cell Biol 8, 310–318.

Santaguida S, Musacchio A (2009). The life and miracles of kinetochores. EMBO J 28, 2511–2531.

Skibbens RV, Rieder CL, Salmon ED (1995). Kinetochore motility after severing between sister centromeres using laser microsurgery: evidence that kinetochore directional instability and position is regulated by tension. J Cell Sci 108, 2537–2548.

Skibbens RV, Salmon ED (1997). Micromanipulation of chromosomes in mitotic vertebrate tissue cells: tension controls the state of kinetochore movement. Exp Cell Res 235, 314–324.

Skibbens RV, Skeen VP, Salmon ED (1993). Directional instability of kinetochore motility during chromosome congression and segregation in mitotic newt lung cells: a push-pull mechanism. J Cell Biol 122, 859–875.

Stumpff J, von Dassow G, Wagenbach M, Asbury C, Wordeman L (2008). The kinesin-8 motor Kif18A suppresses kinetochore movements to control mitotic chromosome alignment. Dev Cell 14, 252–262.

Tirnauer JS, Canman JC, Salmon ED, Mitchison TJ (2002). EB1 targets to kinetochores with attached, polymerizing microtubules. Mol Biol Cell 13, 4308–4316.

VandenBeldt KJ, Barnard RM, Hergert PJ, Meng X, Maiato H, McEwen BF (2006). Kinetochores use a novel mechanism for coordinating the dynamics of individual microtubules. Curr Biol 16, 1217–1223.

Varga V, Helenius J, Tanaka K, Hyman AA, Tanaka TU, Howard J (2006). Yeast kinesin-8 depolymerizes microtubules in a length-dependent manner. Nat Cell Biol 8, 957–962.

Vladimirou E, Harry E, Burroughs N, McAinsh AD (2011). Springs, clutches and motors: driving forward kinetochore mechanism by modelling. Chromosome Res 19, 409–421.

Wan X *et al.* (2009). Protein architecture of the human kinetochore microtubule attachment site. Cell 137, 672–684.

Waters JC, Mitchison TJ, Rieder CL, Salmon ED (1996a). The kinetochore microtubule minus-end disassembly associated with poleward flux produces a force that can do work. Mol Biol Cell 7, 1547–1558.

Waters JC, Skibbens RV, Salmon ED (1996b). Oscillating mitotic newt lung cell kinetochores are, on average, under tension and rarely push. J Cell Sci 109, 2823–2831.

Wordeman L, Wagenbach M, von Dassow G (2007). MCAK facilitates chromosome movement by promoting kinetochore microtubule turnover. J Cell Biol 179, 869–879.

Zhai Y, Kronebusch PJ, Borisy GG (1995). Kinetochore microtubule dynamics and the metaphase-anaphase transition. J Cell Biol 131, 721–734.

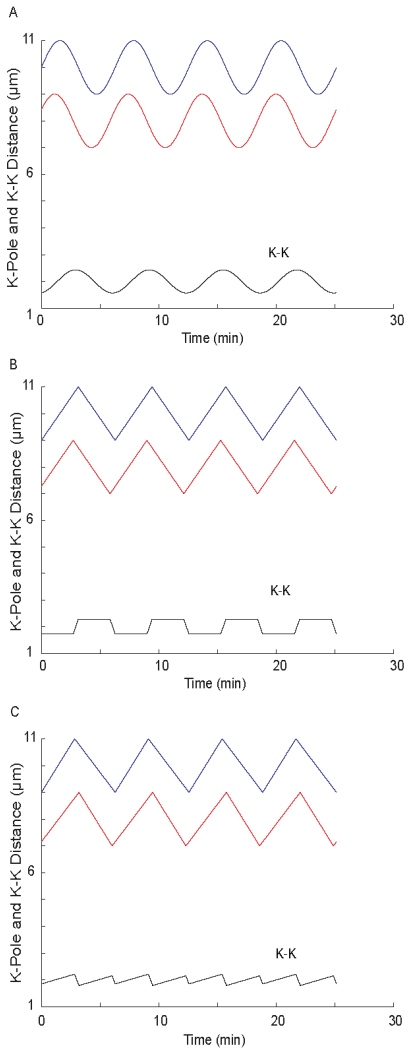

Supplemental Figure 1

Supplemental Figure 1. Oscillation simulations
The amplitude and period of oscillation were made equal to the average value in PtK1 cells. Blue and red lines represent the distance between pole and kinetochore for a sister pair. Black lines are the K-K distance. Simulation of oscillations by sine wave (A) and symmetrical triangular wave (B). In either case, the oscillation frequencies are equal between K-P distance and K-K distance and the phase difference between the sister pair does not change the frequency of K-K distance oscillation. (C) Simulation of oscillation by asymmetric triangle wave with the two kinetochores moving out of phase by about 180 degrees as occurs in vivo. The asymmetry between P and AP movements are similar to the PtK1 oscillation in vivo. The frequency of K-K oscillation is doubled.

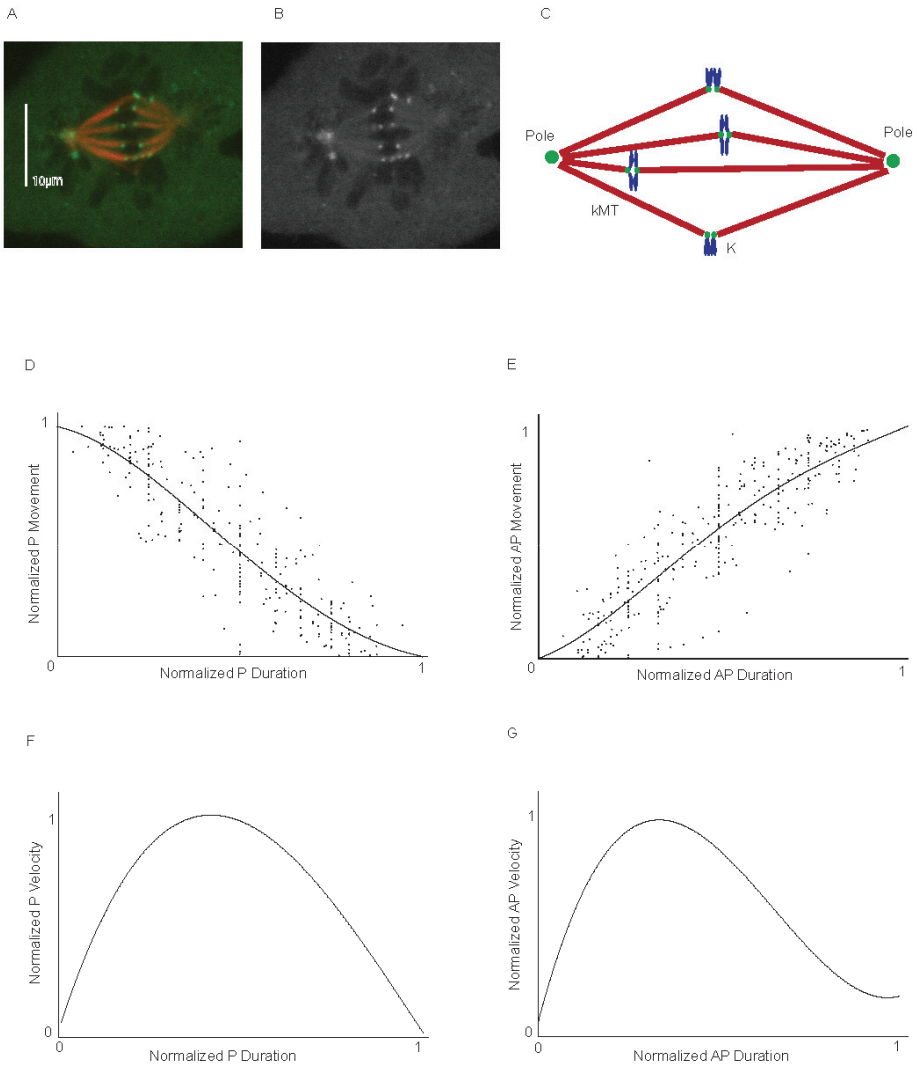

Supplemental Figure 2

Supplemental Figure 2. Measurements of kinetochore and centromere oscillations for normally bioriented chromosomes in late prometaphase spindles.
A-C as in Figure 1 and D-G as described in Figure 4 legend for normally bioriented chromosomes in metaphase spindles. (number of cells: 6; number of sister kinetochore pairs: 12)

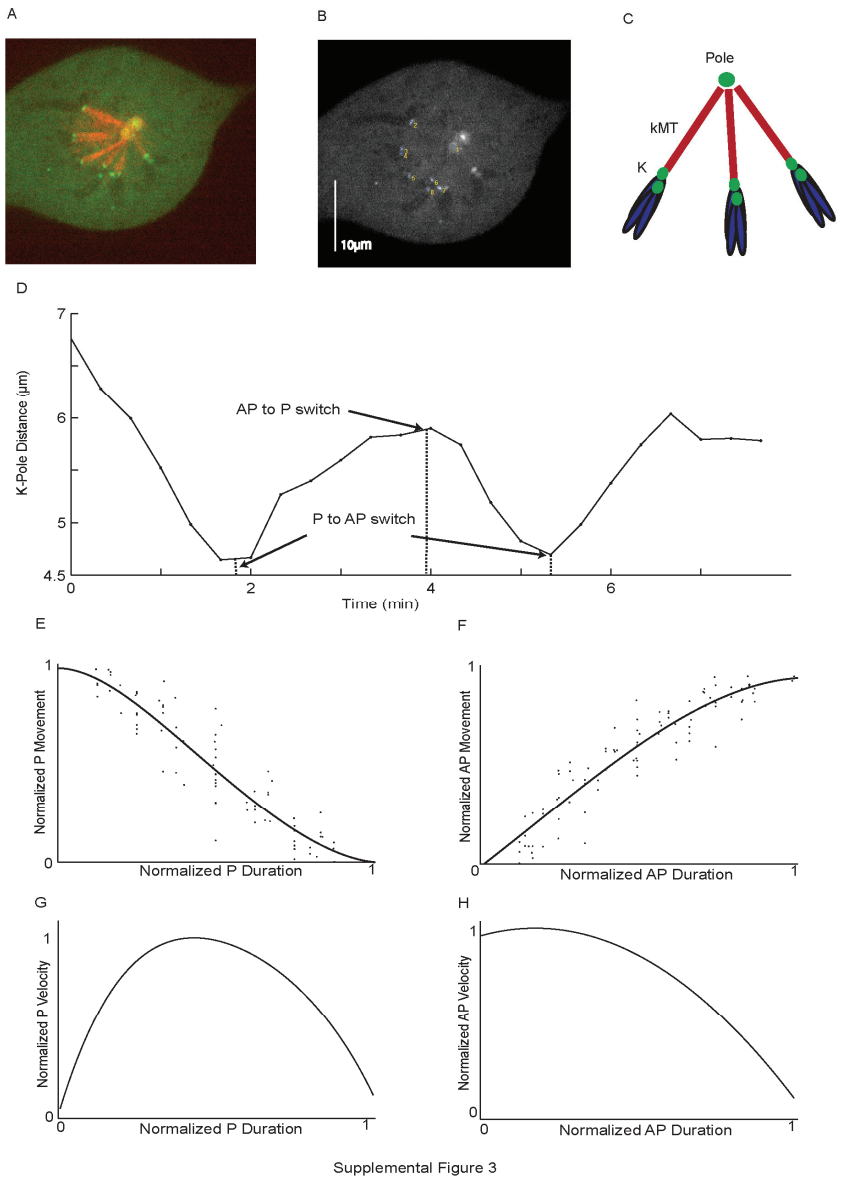

Supplemental Figure 3. Oscillations of mono-oriented chromosomes in monopolar spindles.

A-D as in Figure 1 and D-G as described in Figure 4 legend for normally bioriented chromosomes in metaphase spindles. In these studies, cells assembled monopolar spindles as they entered mitosis in the presence of 100 - 200 μM monastrol, which inhibits the kinesin-5 motor that normally functions to push the poles apart. The average kMT flux in these monopoles, is slightly reduced (0.5 μm/min) in comparison to the rate (0.65 μm/min) typical of metaphase bipolar spindles (Cameron *et al.*, 2006). We did not assay chromosomes with both kinetochores attached to MTs from the pole (syntelic attachments) because asynchrony that is typical near the end of P and AP movements could complicate the analysis (e.g., one moving P while the other is moving AP). (number of cells: 6; number kinetochores: 8)

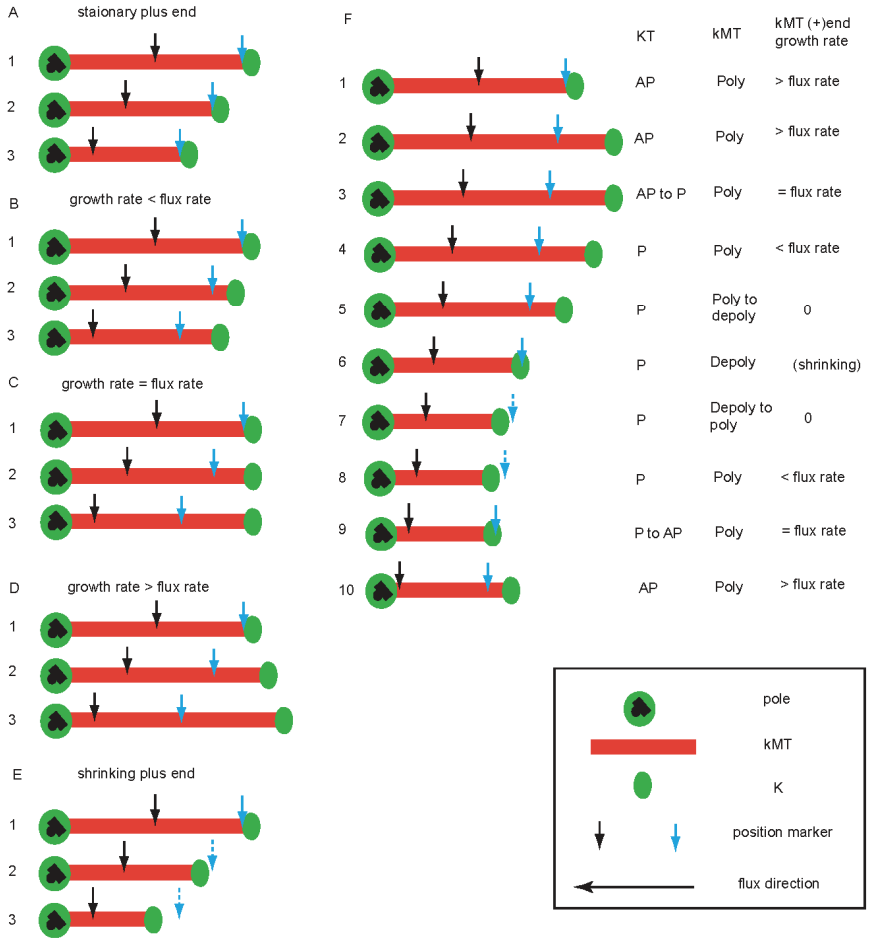

Supplemental Figure 4

Supplemental Figure 4. Schematic diagrams of kMT plus-end dynamic instability and kinetochore dynamic instability with poleward flux.
(A) When there is no kMT plus-end activity, the kinetochore moves poleward with flux. (B) When the plus-end polymerization rate is smaller than the flux rate, the kinetochore is in P motion, P movement velocity equals to the flux rate minus the growth rate. (C) When the polymerization rate is equal to the flux rate, the kinetochore remains stationary. (D) When the polymerization rate is greater than the flux rate, the kinetochore is in AP motion; the AP movement velocity is equal to the polymerization rate minus the flux rate. (E) When the kMT plus-end is depolymerizing, the kinetochore is in P motion; the P movement velocity is equal to the depolymerization rate plus the flux rate. (F) Kinetochore staying in P or AP state is influenced by the kMT plus-end polymerization rate and the flux rate. Black and blue arrows mark the same spots on kMT at different time points; they move with the flux. Labels 1 – 10 represent the same time points indicated in Figure 5.